Crosstalk between 2 organelles: Lysosomal storage of heparan sulfate causes mitochondrial defects and neuronal death in mucopolysaccharidosis III type C

Alexey V Pshezhetsky*

CHU Ste-Justine and Departments of Pediatrics and Biochemistry; University of Montreal; Montreal, QC, Canada

*Correspondence to: Alexey V Pshezhetsky; Email: alexei.pchejetski@umontreal.ca

More than 30% of all lysosomal diseases are mucopolysaccharidoses, disorders affecting the enzymes needed for the stepwise degradation of glycosaminoglycans (mucopolysaccharides). Mucopolysaccharidosis type IIIC (MPS IIIC) is a severe neurologic disease caused by genetic deficiency of heparan sulfate acetyl-CoA: α-glucosaminide N-acetyltransferase (HGSNAT). Through our studies, we have cloned the gene, identified molecular defects in MPS IIIC patients and most recently completed phenotypic characterization of the first animal model of the disease, a mouse with a germline inactivation of the *Hgsnat* gene.[1] The obtained data have led us to propose that Hgsnat deficiency and lysosomal accumulation of heparan sulfate in microglial cells followed by their activation and cytokine release result in mitochondrial dysfunction in the neurons causing their death which explains why MPS IIIC manifests primarily as a neurodegenerative disease. The goal of this addendum is to summarize data yielding new insights into the mechanism of MPS IIIC and promising novel therapeutic solutions for this and similar disorders.

Genetic Diseases of Heparan Sulfate Degradation and MPS IIIC

Heparan sulfate (HS) is a repeating disaccharide comprised of units of sulfated L-iduronic or glucuronic acid linked to N-glucosamine. HS is found in proteoglycans associated with the cell membrane in nearly all cells, but is most abundant in connective tissues and intracellular matrix where is has been shown to play crucial roles in cellular interactions and signaling.[2] Stepwise degradation of HS occurs within the lysosomes by the concerted action of at least 8 enzymes: 4 sulfatases, 3 exoglycosidases and one N-acetyltransferase, which work sequentially at the terminus of HS chains, producing free sulfate and monosaccharides.

The most biochemically intriguing of the enzymes of HS catabolism is heparan sulfate acetyl-CoA: α-glucosaminide N-acetyltransferase (HGSNAT), which catalyzes the only known synthetic reaction in the lysosome. The enzyme is critical to generate the acetylated version of glucosamine because there is no enzyme that can act on the unacetylated molecule. Since the acetyl donor, acetyl-CoA (AcCoA), is not stable in the lysosomal environment,[3] HGSNAT catalyzes the acetylation of HS via a transmembrane reaction.[4]

Seven lysosomal storage diseases are caused by genetic deficiencies of the enzymes involved in HS catabolism. Three of them: MPS I (Hurler-Scheie syndrome, α-iduronidase deficiency), MPS II (Hunter syndrome, iduronate sulfatase deficiency), and MPS VII (Sly syndrome, glucuronidase deficiency) also have blocks in dermatan sulfate degradation and therefore cause accumulation of both compounds. Defects in the remaining 4 enzymes, α-N-acetylglucosaminidase, heparan N-sulfatase, HGSNAT and N-acetylglucosamine 6-sulfatase, uniquely block the catabolism of HS. They are classified as variants of a single disorder, MPS III or Sanfilippo syndrome[5]: MPS III type A (deficiency of

heparan N-sulfatase); MPS III type B (deficiency of α-N-acetylglucosamini- dase); MPS III type C (deficiency of HGSNAT)[6]; and MPS III type D (defi- ciency of N-acetylglucosamine 6-sulfa- tase). All subtypes have similar clinical phenotypes with onset in infancy or early childhood: progressive and severe neurological deterioration causing hyper- activity, sleep disorders and loss of speech accompanied by behavioral abnormalities, neuropsychiatric prob- lems, mental retardation, hearing loss, and visceral manifestations, such as mild hepatomegaly, joint stiffness, femoral head necrosis, biconvex dorsolumbar vertebral bodies, mild coarse faces, and hypertrichosis.[7] Most patients become demented and die before adulthood but some survive to the fourth decade with progressive dementia and retinitis pig- mentosa.[7,8] MPS IIIC contributes to about 25% of all Sanfilippo cases but the disease has higher birth prevalence in some countries such as Portugal and the Netherlands where it's frequency was estimated as 0.12 and 0.21 per 100,000 births respectively.[9,10]

Identification of the MPS IIIC gene and molecular defects in MPS IIIC patients

Despite being the topic of considerable investigation, for many years the isolation and cloning of HGSNAT has been ham- pered by its low tissue content, instability, and hydrophobic nature. We mapped the gene responsible for MPS IIIC to an 8.3- cM interval of chromosome 8[11,12] (further reduced to a 2.6 cM interval between D8S1051 and D8S1831[13]) and identified it as the *TMEM76* (currently *HGSNSAT*) gene which product had 11 predicted transmembrane domains and 4 potential N-glycosylation sites.[13] Independently the *HGSNAT* gene was identified by compa- rable proteomic analysis of the lysosomal membrane.[14]

The cloning of the *HGSNAT* gene paved the way for identification of molec- ular defects in MPS IIIC patients: a total of 63 mutations affecting almost all 18 exons and many introns of the gene in MPS IIIC patients were reported by us[13,15,16] as well as by others.[14,17,18] All variants are currently listed in a locus

specific online database (LSDB) at http:// chromium.liacs.nl/LOVD2/home.php? select_db=HGSNAT. The spectrum of mutations in MPS IIIC patients shows high heterogeneity, but some identified mutations have high frequency within a population suggesting founder effects, such as in the Netherlands,[15] Italy[17] or Portugal[18] whereas several mutations were common across populations.

MPS IIIC as a protein missfolding disease

Identification of the molecular defects in MPS IIIC gave rise to a question why the patients bearing missense mutations (identified in about 50% of cases) all have clinical phenotype as severe as in those affected with splice, frameshift or non- sense mutations completely abolishing production of the protein. To answer this we studied catalytic activity, oligomeric structure and biogenesis of HGSNAT and its mutants.[19,20] Our results showed that HGSNAT is synthesized as a catalytically inactive 78-kDa precursor transported to the lysosomes via an adaptor protein- mediated pathway involving tyrosine and dileucine-based conserved lysosomal tar- geting signals in its C-terminal cyto- plasmic domain with a contribution of a dileucine-based signal in the N-terminal cytoplasmic loop. In the lysosome the pre- cursor is cleaved into a 29-kDa N-termi- nal α-chain and a 49-kDa C-terminal β-chain held together by disulfide bonds between cysteine residues in its lysosomal luminal loops and assembled into 440- kDa tetramers. This proteolytic cleavage allows acetyl-CoA to access the enzyme active site and acetylate the nucleophilic residue His269 for further transfer of the acetyl group to the glucosamine group on HS.[19] Interestingly, the follow up study by Fan et al.[21] while confirming that the HGSNAT precursor is processed into a small N-terminal and a larger C-terminal chains, reported that this cleavage and oligomerization were not necessary for activation of the enzyme, since the puri- fied precursor of recombinant HGSNAT showed some enzymatic activity. Fan et al. also reported that according to their kinetic data the catalytic mechanism of the enzymatic reaction involved formation of a ternary complex between the enzyme,

AcCoA and HS. While direct structural studies are necessary to understand how HGSNAT functions and how it is proc- essed and assembled, our hypothesis that HGSNAT is activated through intralyso- somal proteolytic cleavage is indirectly supported by the results of the expression analysis of the 18 HGSNAT mutants rep- resenting all identified to date missense MPS IIIC mutations.[20] All expressed HGSNAT mutants were abnormally gly- cosylated and retained in the endoplasmic reticulum instead of being targeted to the lysosome suggesting that they lack a nor- mal protein fold. All mutants were also missing proteolytic processing. These results showed that the enzyme folding defects due to missense mutations, together with nonsense-mediated mRNA decay, are the 2 major molecular mecha- nisms underlying MPS IIIC[20] and point to the important role that impairment of normal protein folding plays in develop- ment of clinical symptoms in MPS III. Storage of missfolded protein aggregates has been reported in the brains of knock- out mouse model of MPS IIIB,[22,23] although the molecular basis of this accu- mulation still remains the subject of dis- cussion since other reports did not detect signs of the ER stress or impaired protea- somal activity in the same model.[24,25] Nevertheless it is tempting to speculate that the accumulation of missfolded HGSNAT in the cells of patients affected with missense mutations may cause a dominant effect stressing ER-associated protein degradation machinery and affect- ing general protein degradation pathways and cell homeostasis. Comparative study of the brain pathology in *Hgsnat* knockout mouse model and those expressing missfolded HGSNAT protein would be instrumental for clarifying this issue.

Generation, biochemical validation and phenotypic characterization of the MPS IIIC mouse model

Important insights into the physiologi- cal mechanism underlying the develop- ment of clinical symptoms in MPS IIIA and B have been provided by studying ani- mal models of the disease, principally the 2 mouse models: a knockout mouse model of MPS IIIB[26] and a spontaneous mouse model of MPS IIIA.[27] Since no

animal models existed for MPS IIIC, we used gene trap technology to generate a functional knockout of the *Hgsnat* locus in C57Bl/6N mice.[1] A cassette containing a fusion between the β-galactosidase and neomycin resistance genes (β-geo selectable marker) was inserted into the intron 7 of the *Hgsnat* gene, generating a nonfunctional *Hgsnat* fusion transcript.

Hgsnat mRNA expression and level of HGSNAT activity in multiple tissues and in cultured skin fibroblasts from the homozygous for the *Hgsnat-Geo* allele animals (*Hgsnat-Geo* mice) were reduced to 0.6–1.5% as compared to WT confirming the efficiency of the splicing and validating the model biochemically.

Hgsnat-Geo mice were viable, had normal growth and did not present symptoms of the disease until the age of 11–12 months when they started showing weight loss, loss of fur and abnormal gait. About 30% of animals at this age showed spasticity of hind limbs and loss of coordination in a balance test. At ~65 weeks of age mice presented signs of urinary retention resulting in abdominal distension (absent in human patients but present in the mouse models of both MPS IIIA and

MPS IIIB[22,27]) and had to be euthanized. The mean lifespan of *Hgsnat-Geo* mice was around 65 weeks, about half of that of WT C57Bl/6J mice (**Fig. 1**).

Increased activity and reduced anxiety (i.e. higher than average speed and distance traveled, increased frequency of crossing the central field and central distance traveled, as well as decreased frequency and duration of periods of immobility) was detected by open field test at 8 months of age (**Fig. 1**). By the age of 10 months the signs of hyperactive behavior diminished resembling the trend observed in human patients.

Defects in hippocampal function were detected at 10 months by the Morris Water Maze test to measure memory and spatial learning capability. The learning progress of mutant mice at the ages of 5, 7 and 8 months was similar to that of their WT counterparts, whereas at the age of 10 months, *Hgsnat-Geo* mice needed significantly more time to find the hidden platform, suggesting impaired spatial learning (**Fig. 1**). Additionally, when the platform was removed, HGSNAT-deficient mice spent significantly less time and traveled less distance than WT mice in the target quadrant where the platform used

to be located, which indicated a decline of spatial memory. To summarize, the clinical symptoms in *Hgsnat-Geo* mice start at 6–8 months with hyperactivity, and reduced anxiety; cognitive memory decline becomes apparent at 10 months and at 12–13 months mice show signs of unbalanced gait and urinary retention (**Fig. 1**).

Brain pathology in MPS IIIC mice

To elucidate the pathophysiological mechanism underlying behavioral abnormalities we analyzed brain structure by light and electron microscopy. In contrast to human MPS III patients who show rapid neurodegeneration[28] mouse brain cortex had normal stratification even at the age of 12 months suggesting the absence of massive neurodepletion. However, by quantifying NeuN-stained neurons in somatosensory cortex we showed that neuronal loss in homozygous *Hgsnat-Geo* mice actually occurs starting from the age of 10 months and results by the age of 12 months in the >30% reduction of neuronal density (**Fig. 2A**). In the cerebellar cortex, Purkinje cell loss was also substantial by 12 months, especially in the anterior lobe (**Fig. 2B**). In contrast
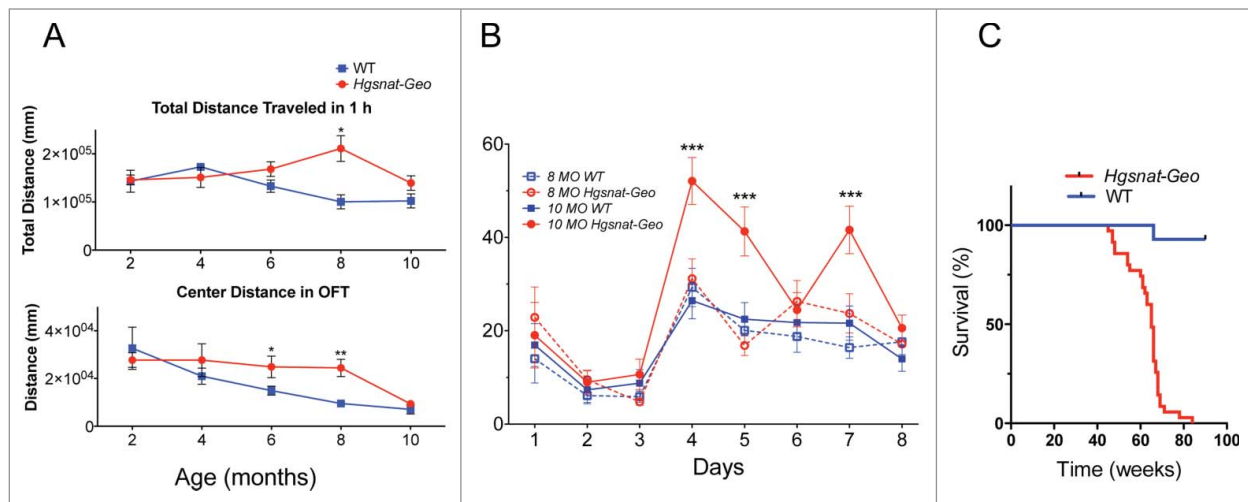

Figure 1. Disease progression in *Hgsnat-Geo* mice. (**A**) Six and 8-month-old *Hgsnat-Geo* female mice show signs of hyperactivity and reduced anxiety compared to WT mice as detected by open field test performed 1 h into their light cycle. Increased activity (total distance traveled) was detected at 8 months. Reduced anxiety (increased center activity) was detected at 6 and 8 months. P value was calculated by 2-way-ANOVA (*$P < 0.05$, **$P < 0.01$). From 6 (2, 4 and 6 month old) to 10 (8 and 10 month old) naïve mice were studied per age/per genotype. (**B**) *Hgsnat-Geo* mice ($N = 6$; 3 males, 3 females) showed impaired performance in the spatial memory-based Morris Water Maze test at 10 months. All mice showed similar average latencies on days 1–3 of visible platform testing. Whereas 8-month-old *Hgsnat-Geo* mice had latencies in the hidden platform testing similar to those of their wild type counterparts (days 4–8), 10-month-old mutant mice were significantly impaired in this spatial learning test. (**C**). Kaplan-Meier plot showing survival of *Hgsnat-Geo* mice ($N = 50$; 25 males, 25 females) and their wild type counterparts ($N = 70$; 35 males, 35 females). By the age of 70 weeks the vast majority of *Hgsnat-Geo* mice died or had to be euthanized on the veterinarian request due to urinary retention.
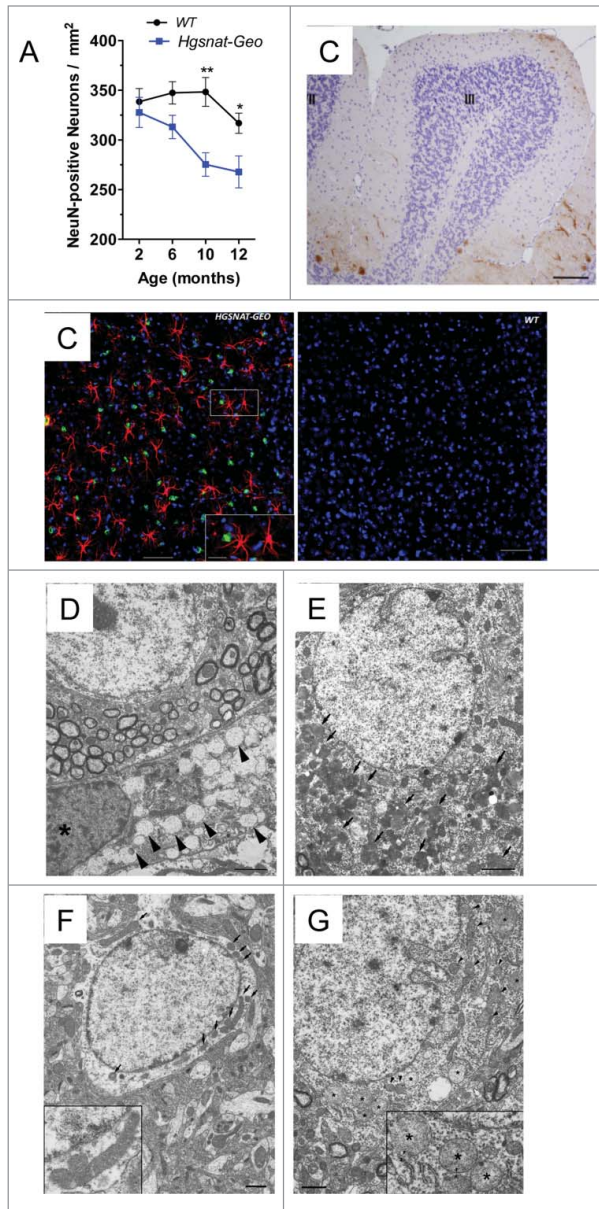
Figure 2. Pathological changes in the brains of *Hgsnat-Geo* mice. (**A**) Progressive loss of neurons in somatosensory cortex. NeuN-positive neurons were counted in 2 adjacent fields on 3 sagittal sections (1.44, 1.68 and 1.92 mm from bregma) of S1 somatosensory cortex; 2 male and 2 female mice were studied for each age and each genotype. Two-way repeated measurements ANOVA was used to test differences between the mouse groups: significant differences between the mean values in Bonferroni post-test (*$P < 0.05$, **$P < 0.001$, ***$P < 0.0001$) are shown. (**B**) Purkinje cells are largely absent in the lobule III of the anterior cerebellar lobe of Hgsnat-Geo mouse at the age of 12 months. H&E staining. Bar represents 50 μm. (**C**) Increased numbers of GFAP-positive astrocytes (red) and CD68-positive microglia (green) are detected in the somatosensory cortex of 4 months-old *Hgsnat-Geo* mice. (**D**) Storage pattern in microglia detected at 5 months. Massive accumulation of vacuoles with single limiting membranes and a sparse fine content in the cytoplasm is compatible with lysosomal GAG storage. Lysosomes containing storage materials are marked by arrowheads. The microglial cell (nucleus is marked by an asterisk) is in a close proximity to a cortical brain neuron. Bar represents 2 μm. (**E**) Lysosomal system in a cortical neuron at 12 months is expanded and massively overloaded by electron dense material (marked by arrows). Bar represents 2 μm. (**F**) Mitochondrial population in neurons of WT mice at the age of 12 months is relatively uniform and is composed of normally shaped mitochondria with largely regular cristae (details are shown in the insert). Bar represent 1 μm. (**E**) At the age of 12 months mitochondria in neurons of *Hgsnat-Geo* mice are displaying swelling and disorganization of their inner membranes (marked by arrowheads). Edematous mitochondria with largely dissolved cristae are marked by asterisks. Insert shows a detailed view of highly edematous mitochondria with remnants of double membranes (marked by double arrowheads). Bar represents 1 μm.

gradually increasing levels of activated isolectin B4/CD68-positive microglia cells and GFAP-positive astrocytes were detected throughout the brain (**Fig. 2C**). Together with increased expression of inflammation markers, MIP1α (CCL3) and TNFα[1] these data were consistent with progressive neuroinflammation in *Hgsnat-Geo* mice.

Multiple CD68-positive foam microglia cells with storage vacuoles were present in both gray and white matter being most prominent in caudoputamen and brain cortex. Presence of storage materials in microglia was detected as early as at 2 months of age and seemed to be the initial pathological event in the brain preceding pathological changes in neurons. Storage in microglia further increased with age.

In neurons progressive cytoplasmic accumulation of autofluorescent granular material was observed in all examined brain regions. At 5 months storage was restricted to individual neurons but at 12 months it affected the whole neuronal population especially the cells in deep cortical layers, hippocampus and cerebellum. At the ultrastructural level, neurons showed progressive lysosomal accumulation of closely packed fibrillary deposits of a rectilinear and/or fingerprint type resembling those detected in neuronal ceroid lipofuscinoses and different from storage vacuoles in microglia, which had a uniform electron-lucent appearance (**Fig. 2D, E**). Similar heterogeneous storage and the presence of "fingerprint-like" structures identified as the aggregates of the subunit C of mitochondrial ATP synthase (SCMAS) were previously reported for other MPS mouse models.[29,30] At the most advanced stages of the disease (14–16 months), these deposits became the dominant ultrastructural pattern in neuronal lysosomes. Besides, individual neurons underwent severe regressive changes.

Materials stored in the brain cells were further studied by immunohistochemistry. HS storage was detected in the lysosomes of multiple NeuN-positive neurons, but most of HS storage was detected in activated foam microglia cells positive for isolectin B4 and CD68. G_{M2} and G_{M3} gangliosides, almost undetectable in the brain of WT mice were highly present in

the neurons in most brain areas of *Hgsnat-Geo* mice. The highest number of ganglioside-storing neurons was found in deep layers of cortex and hippocampus and in contrast to HS accumulation it dramatically increased with age. Stored gangliosides only partially co-localized with lysosomal marker LAMP-1 suggesting that they were also accumulated in the compartments having non-lysosomal origin. Similarly to neurons of MPS IIIA and MPS IIIB mouse models[22,23] neurons of *Hgsnat-Geo* mice also contained SCMAS aggregates, increased levels of ubiquitin and protein markers of Alzheimer disease and other tauopathies such as lysozyme, hyperphosphorylated tau (Ptau), Ptau kinase, Gsk3β, and β amyloid suggestive of mitophagy and a general impairment of proteolysis. Indeed, starting from 6 months of age increased levels of LC3-phosphatidylethanolamine conjugate (LC3-II) were detected in brain tissues indicating increased autophagosomal genesis or decreased macroautophagic flux. We also detected increased levels of O-GlcNAc-modified proteins, an indication of the ER stress often associated with impaired cellular proteolysis.[31]

Progressive mitochondrial pathology in the neurons of MPS IIIC mice

One of the most striking pathological changes in neurons observed in all parts of the brain was progressive mitochondrial damage. Mitochondria were pleomorphic and increased in number; many of them were swollen and contained disorganized cristae or reduced number of cristae. In contrast no structural changes were observed in the mitochondria of microglial cells. Neurons containing swollen mitochondria were present as early as at 5 month of age, and by the age of 12 months the mitochondrial damage was observed in the majority of neurons (**Fig. 2F, G**). Besides, the mitochondrial network was less organized and the ratio between the fused and single mitochondria was reduced in the neurons of *Hgsnat-Geo* mice as compared with WT mice. High degree of co-localization was observed between mitochondria and stored gangliosides suggesting that some of the ganglioside-storing granules could

appear in the result of impaired mitophagy.

Consistent with the progressive mitochondrial defects observed by light and electron microscopy, activities of complex IV (COX) and complex II (SQR) mitochondrial enzymes and the total content of coenzyme Q10 in the brain tissues were significantly lower in Hgsnat-Geo mice than in the corresponding WT controls at the ages of 8 and 12 months, respectively. Besides, the activities of complex II (SQR), complex II+III (SCCR) and citrate synthase in *Hgsnat-Geo* mice decreased significantly with age, whereas no such dependence was detected for the WT animals.

Putative mechanism underlying neurodegeneration in the MPS IIIC mice

Further studies are necessary to determine the precise sequence of events that leads to a widespread brain pathology and neuronal death in MPS IIIC. Our results however allow hypothesizing that the malfunction and loss of neurons can be at least partially mediated by pathological changes in their mitochondrial system. We speculate that accumulation of HS and HS-derived oligosaccharides in

microglia is the primary pathological event that triggers a cascade of downstream reactions. HS-derived oligosaccharides presumably released by exocytosis of lysosomes are known to induce general inflammation reactions in the brain by activating TLR receptors of microglia cells, resulting in release of multifunctional cytokines such as TNF-α and MIP-1-α. We speculate that these cytokines known to cause mitochondrial damage through formation of ROS and oxidative stress[32-34] eventually lead to neuronal death observed in somatosensory cortex and cerebellum in MPS IIIC mice and dominant in all brain regions of MPS III patients[28] (**Fig. 3**). Progressive accumulation of ganglioside and ceroid-type densely packed protein aggregates detected in neurons at the advanced stage of the disease can also be partially of mitochondrial origin due to mitophagy and impaired catabolism of autophagosomal content. While out data suggest autophagic alterations in the brain cells of *Hgsnat-Geo* mouse, it remains to be determined whether autophagy is indeed impaired since the detected LC3-II accumulation can reflect both increased autophagy or defective proteolysis following formation
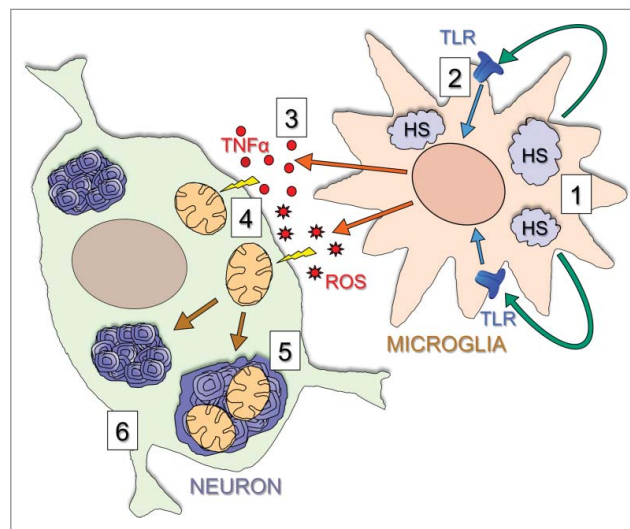

Figure 3. Proposed mechanism underlying brain disease in Hgsnat-Geo mice. The disease starts with accumulation of HS and HS-derived oligosaccharides in microglial cells (**1**). Through their release by exocytosis of lysosomes and action on TLR receptors (**2**) these materials induce general inflammation reactions in the brain, including the release of multifunctional cytokines such as TNFα and MIP-1α (**3**). The cytokines cause mitochondrial damage (**4**), and together with primary storage contribute to autophagy block and secondary storage of gangliosides and missfolded proteins in neurons (**5**) eventually leading to neuronal death in critical areas (**6**).

of the autophagosome. Further studies are also necessary to determine if progressive neuroinflammation/mitochondrial dysfunction, which we defined here for MPS IIIC may represent a common phenomenon for metabolic neurodegenerative diseases.

Potential implications for therapy of MPS IIIC patients

Currently, there is no specific treatment for MPS IIIC and since the CNS is the major affected organ and the deficient HGSNAT is a multi-span transmembrane protein, it is unlikely that enzyme replacement can be effective for treating this disorder, leaving gene therapy, chaperone therapy (for patients affected with missense mutations) and substrate reduction therapy as potentially suitable approaches. For 5 missense mutations in MPS IIIC we could partially rescue the mutant misfolded enzyme by treating patient's cells with the competitive inhibitor of HGSNAT, glucosamine.[16] These "responding" mutations are among the most frequent, so the majority of known MPS IIIC patients are affected with at least one of them. The effect of glucosamine in most cases was relatively modest, i.e., the restored level of enzyme activity was below that in the normal control cells, probably because glucosamine is a relatively weak inhibitor of HGSNAT,[16] but other more potent chaperones could probably produce enough enzyme in the patient's cells to reverse the HS storage.

The analysis of MPS IIIC mouse model showing that pathological changes in the brain start from storage of HS in microglia followed by their activation and cytokine release, suggests that patients with MPS IIIC can eventually benefit from a gene therapy approach based on correcting the deficient enzyme activity in monocyte/macrophage cells via lentivirus-mediated targeting of the HGSNAT gene into haematopoietic stem/progenitor cells (HSPC), followed by their transplantation. This procedure should eventually populate the brain with microglia overexpressing HGSNAT, stop storage of toxic HS species in microglia and reduce inflammation. This could slow down the neuronal death and potentially improve clinical phenotype. Since microglia are derived from HSPC, they are the only brain cells that can be readily targeted without performing difficult, expensive, and potentially dangerous stereotactic or intrathecal delivery of the virus. Most importantly, targeting monocyte/macrophage lineages offers not only correction of the enzymatic and metabolic defect but also correction of the secondary abnormalities related to dysfunction of engorged macrophages such as production of inflammatory cytokines, ROS, and other tissue-damaging stimuli, thus breaking a vicious cycle: storage $\rightarrow$ dysfunction $\rightarrow$ recruitment/activation of further macrophages $\rightarrow$ increased storage. If confirmed this approach may provide a paradigm for therapeutic interventions in other neurodegenerative disorders involving brain inflammation.

Disclosure of Potential Conflicts of Interest

No potential conflicts of interest were disclosed.

References

1. Martins C, Hulkova H, Dridi L, Dormoy-Raclet V, Grigoryeva L, Choi Y, Langford-Smith A, Wilkinson FL, Ohmi K, DiCristo G, et al. Neuroinflammation, mitochondrial defects and neurodegeneration in mucopolysaccharidosis III type C mouse model. Brain 2015; 138:336-55; PMID:25567323; http://dx.doi.org/10.1093/brain/awu355

2. Gallagher JT. Multiprotein signalling complexes: regional assembly on heparan sulphate. Biochem Soc Trans 2006; 34:438-41; PMID:16709181; http://dx.doi.org/10.1042/BST0340438

3. Rome LH, Hill DF, Bame KJ, Crain LR. Utilization of exogenously added acetyl coenzyme A by intact isolated lysosomes. J Biol Chem 1983; 258:3006-11; PMID:6402508

4. Bame KJ, Rome LH. Acetyl coenzyme A: alpha-glucosaminide N-acetyltransferase. Evidence for a transmembrane acetylation mechanism. J Biol Chem 1985; 260:11293-9; PMID:3897232

5. Sanfilippo SJ, Podosin R, Langer L, Good RA. Mental retardation associated with acid mucopolysacchariduria (heparitin sulfate type). J Pediatr; 63:837-8; http://dx.doi.org/10.1016/S0022-3476(63)80279-6

6. Klein U, Kresse H, von Figura K. Sanfilippo syndrome type C: deficiency of acetyl-CoA:alpha-glucosaminide N-acetyltransferase in skin fibroblasts. Proc Natl Acad Sci U S A 1978; 75:5185-9; PMID:33384; http://dx.doi.org/10.1073/pnas.75.10.5185

7. Neufeld EF, Muenzer J. The Mucopolysaccharidoses. In: The Metabolic and Molecular Basis of Inherited Disease. Scriver CR, Beaudet AL, Sly WS, Valle D. eds. USA, New-York: McGraw-Hill, 2001:3421-52.

8. Valstar MJ, Ruijter GJ, van Diggelen OP, Poorthuis BJ, Wijburg FA. Sanfilippo syndrome: a mini-review. J Inherit Metab Dis 2008; 31:240-52; PMID:18392742; http://dx.doi.org/10.1007/s10545-008-0838-5

9. Pinto R, Caseiro C, Lemos M, Lopes L, Fontes A, Ribeiro H, Pinto E, Silva E, Rocha S, Marcao A, et al. Prevalence of lysosomal storage diseases in Portugal. Eur J Hum Genet 2004; 12:87-92; PMID:14685153; http://dx.doi.org/10.1038/sj.ejhg.5201044

10. Poorthuis BJ, Wevers RA, Kleijer WJ, Groener JE, de Jong JG, van Weely S, Niezen-Koning KE, van Diggelen OP. The frequency of lysosomal storage diseases in The Netherlands. Hum Genet 1999; 105:151-6; PMID:10480370; http://dx.doi.org/10.1007/s004399900075

11. Ausseil J, Loredo-Osti JC, Verner A, Darmond-Zwaig C, Maire I, Poorthuis B, van Diggelen OP, Hudson TJ, Fujiwara TM, Morgan K, et al. Localisation of a gene for mucopolysaccharidosis IIIC to the pericentromeric region of chromosome 8. J Med Genet 2004; 41:941-5; PMID:15591281; http://dx.doi.org/10.1136/jmg.2004.021501

12. Seyrantepe V, Tihy F, Pshezhetsky AV. The microcell-mediated transfer of human chromosome 8 restores the deficient N-acetyltransferase activity in skin fibroblasts of Mucopolysaccharidosis type IIIC patients. Hum Genet 2006; 120:293-6; PMID:16783568; http://dx.doi.org/10.1007/s00439-006-0211-4

13. Hrebicek M, Mrazova L, Seyrantepe V, Durand S, Roslin NM, Noskova L, Hartmannova H, Ivanek R, Cizkova A, Poupetova H, et al. Mutations in TMEM76* cause mucopolysaccharidosis IIIC (Sanfilippo C syndrome). Am J Hum Genet 2006; 79:807-19; PMID:17033958; http://dx.doi.org/10.1086/508294

14. Fan X, Zhang H, Zhang S, Bagshaw RD, Tropak MB, Callahan JW, Mahuran DJ. Identification of the gene encoding the enzyme deficient in mucopolysaccharidosis IIIC (Sanfilippo disease type C). Am J Hum Genet 2006; 79:738-44; PMID:16960811; http://dx.doi.org/10.1086/508068

15. Ruijter GJ, Valstar MJ, van de Kamp JM, van der Helm RM, Durand S, van Diggelen OP, Wevers RA, Poorthuis BJ, Pshezhetsky AV, Wijburg FA. Clinical and genetic spectrum of Sanfilippo type C (MPS IIIC) disease in The Netherlands. Mol Genet Metab 2008; 93:104-11; PMID:18024218; http://dx.doi.org/10.1016/j.ymgme.2007.09.011

16. Feldhammer M, Durand S, Mrazova L, Boucher RM, Laframboise R, Steinfeld R, Wraith JE, Michelakakis H, van Diggelen OP, Hrebicek M, et al. Sanfilippo syndrome type C: mutation spectrum in the heparan sulfate acetyl-CoA: alpha-glucosaminide N-acetyltransferase (HGSNAT) gene. Hum Mutat 2009; 30:918-25; PMID:19479962; http://dx.doi.org/10.1002/humu.20986

17. Fedele AO, Filocamo M, Di Rocco M, Sersale G, Lubke T, di Natale P, Cosma MP, Ballabio A. Mutational analysis of the HGSNAT gene in Italian patients with mucopolysaccharidosis IIIC (Sanfilippo C syndrome). Mutation in brief #959. Online. Hum Mutat 2007; 28:523; PMID:17397050; http://dx.doi.org/10.1002/humu.9488

18. Coutinho MF, Lacerda L, Prata MJ, Ribeiro H, Lopes L, Ferreira C, Alves S. Molecular characterization of Portuguese patients with mucopolysaccharidosis IIIC: two novel mutations in the HGSNAT gene. Clin Genet 2008; 74:194-5; PMID:18518886; http://dx.doi.org/10.1111/j.1399-0004.2008.01040.x

19. Durand S, Feldhammer M, Bonneil E, Thibault P, Pshezhetsky AV. Analysis of the biogenesis of heparan sulfate acetyl-CoA:alpha-glucosaminide N-acetyltransferase provides insights into the mechanism underlying its complete deficiency in mucopolysaccharidosis IIIC. J Biol Chem 2010; 285:31233-42; PMID:20650889; http://dx.doi.org/10.1074/jbc.M110.141150

20. Feldhammer M, Durand S, Pshezhetsky AV. Protein misfolding as an underlying molecular defect in mucopolysaccharidosis III type C. PLoS One 2009; 4:e7434; PMID:19823584; http://dx.doi.org/10.1371/journal.pone.0007434

21. Fan X, Tkachyova I, Sinha A, Rigat B, Mahuran D. Characterization of the biosynthesis, processing and kinetic mechanism of action of the enzyme deficient in

mucopolysaccharidosis IIIC. PLoS One 2011; 6: e24951; PMID:21957468; http://dx.doi.org/10.1371/journal.pone.0024951

22. Ohmi K, Kudo LC, Ryazantsev S, Zhao HZ, Karsten SL, Neufeld EF. Sanfilippo syndrome type B, a lysosomal storage disease, is also a tauopathy. Proc Natl Acad Sci U S A 2009; 106:8332-7; PMID:19416848; http://dx.doi.org/10.1073/pnas.0903223106

23. Ohmi K, Zhao HZ, Neufeld EF. Defects in the medial entorhinal cortex and dentate gyrus in the mouse model of Sanfilippo syndrome type B. PLoS One 2011; 6: e27461; PMID:22096577; http://dx.doi.org/10.1371/journal.pone.0027461

24. Villani GR, Chierchia A, Di Napoli D, Di Natale P. Unfolded protein response is not activated in the mucopolysaccharidoses but protein disulfide isomerase 5 is deregulated. J Inherit Metab Dis 2012; 35:479-93; PMID:22002444; http://dx.doi.org/10.1007/s10545-011-9403-8

25. Settembre C, Fraldi A, Jahreiss L, Spampanato C, Venturi C, Medina D, de Pablo R, Tacchetti C, Rubinsztein DC, Ballabio A. A block of autophagy in lysosomal storage disorders. Hum Mol Genet 2008; 17:119-29; PMID:17913701; http://dx.doi.org/10.1093/hmg/ddm289

26. Li HH, Yu WH, Rozengurt N, Zhao HZ, Lyons KM, Anagnostaras S, Fanselow MS, Suzuki K, Vanier MT, Neufeld EF. Mouse model of Sanfilippo syndrome type

B produced by targeted disruption of the gene encoding alpha-N-acetylglucosaminidase. Proc Natl Acad Sci U S A 1999; 96:14505-10; PMID:10588735; http://dx.doi.org/10.1073/pnas.96.25.14505

27. Bhaumik M, Muller VJ, Rozaklis T, Johnson L, Dobrenis K, Bhattacharyya R, Wurzelmann S, Finamore P, Hopwood JJ, Walkley SU, et al. A mouse model for mucopolysaccharidosis type III A (Sanfilippo syndrome). Glycobiology 1999; 9:1389-96; PMID:10561464; http://dx.doi.org/10.1093/glycob/9.12.1389

28. Shapiro EG, Nestrasil I, Ahmed A, Wey A, Rudser KR, Delaney KA, Rumsey RK, Haslett PA, Whitley CB, Potegal M. Quantifying behaviors of children with Sanfilippo syndrome: The Sanfilippo Behavior Rating Scale. Mol Genet Metab 2015; 114:594-8; PMID:25770355; http://dx.doi.org/10.1016/j.ymgme.2015.02.008

29. Ryazantsev S, Yu WH, Zhao HZ, Neufeld EF, Ohmi K. Lysosomal accumulation of SCMAS (subunit c of mitochondrial ATP synthase) in neurons of the mouse model of mucopolysaccharidosis III B. Mol Genet Metab 2007; 90:393-401; PMID:17185018; http://dx.doi.org/10.1016/j.ymgme.2006.11.006

30. McGlynn R, Dobrenis K, Walkley SU. Differential subcellular localization of cholesterol, gangliosides, and glycosaminoglycans in murine models of mucopolysaccharide storage disorders. J Comp Neurol 2004;

480:415-26; PMID:15558784; http://dx.doi.org/10.1002/cne.20355

31. Chatham JC, Marchase RB. Protein O-GlcNAcylation: A critical regulator of the cellular response to stress. Curr Signal Transduct Ther 2010; 5:49-59; PMID:22308107; http://dx.doi.org/10.2174/157436210790226492

32. Baregamian N, Song J, Bailey CE, Papaconstantinou J, Evers BM, Chung DH. Tumor necrosis factor-alpha and apoptosis signal-regulating kinase 1 control reactive oxygen species release, mitochondrial autophagy, and c-Jun N-terminal kinase/p38 phosphorylation during necrotizing enterocolitis. Oxid Med Cell Longev 2009; 2:297-306; PMID:20716917; http://dx.doi.org/10.4161/oxim.2.5.9541

33. Chen XH, Zhao YP, Xue M, Ji CB, Gao CL, Zhu JG, Qin DN, Kou CZ, Qin XH, Tong ML, et al. TNF-alpha induces mitochondrial dysfunction in 3T3-L1 adipocytes. Mol Cell Endocrinol 2010; 328:63-9; PMID:20667497; http://dx.doi.org/10.1016/j.mce.2010.07.005

34. Vitner EB, Farfel-Becker T, Eilam R, Biton I, Futerman AH. Contribution of brain inflammation to neuronal cell death in neuronopathic forms of Gaucher's disease. Brain 2012; 135:1724-35; PMID:22566609; http://dx.doi.org/10.1093/brain/aws095